16TH EUROPEAN CONFERENCE ON EARTHQUAKE ENGINEERING THESSALONIKI 18 - 21 JUNE 2018

COST BASED DESIGN AND PERFORMANCE OF SUPPLEMENTAL VISCOUS DAMPERS ATTACHED TO NON-CONSECUTIVE FLOORS

Felipe SAITUA[1], Diego LOPEZ-GARCIA[2] and Alexandros TAFLANIDIS[3]

ABSTRACT

The cost-based optimal height-wise distributions of viscous dampers in multistory structures is investigated in this paper emphasizing applications for which the dampers are attached to the main structure in such a way that they are subjected to the motion of a given floor relative to that of a non-consecutive floor (e.g., two or three floors apart) rather than, as usual, to the relative motion between consecutive floors. It is shown under simplifying assumptions that, for a given level of energy dissipation, damping systems in which (linear or nonlinear) dampers are connected every n_c floor levels reduce damper force demands n_c times with respect to dampers attached to consecutive floor levels. Since the cost of the damping system is directly related to these forces, implementation of non-consecutive connectivity schemes could lead, therefore, to significant economic benefits. To investigate this trends under more realistic modeling assumptions, a height-wise damper distribution optimization scheme that explicitly considers cost associated with damper forces is developed. Seismic excitation is modeled as a stochastic process, and response statistics are obtained through state-space analysis. Different objective functions related to damper forces are adopted, whereas structural performance is incorporated in the design as a constraint, requiring that a specific level of vibration suppression be achieved through the damper implementation. The design of a supplemental viscous damping system for an actual Chilean 26-storey building considering an excitation that is compatible with the regional seismic hazard is examined as illustrative example. Comparisons between consecutive and non-consecutive bracing schemes demonstrate that dampers connected across multiple floors contribute to considerable reduction for the damper force demand.

Keywords: viscous dampers; non-consecutive connectivity; damper cost; distribution optimization

1. INTRODUCTION

Fluid viscous dampers are an attractive seismic protection device for new and existing buildings (Symans et al. 2008). Their effectiveness in reducing the seismic response of multistorey buildings is sensitive to their chosen distribution (Singh and Moreschi 2002; Whittle et al. 2012), and a variety of optimization approaches, considering different performance quantifications and modeling assumptions, have been developed for this task (Zhang and Soong 1992; Takewaki 1997; Lopez-Garcia 2001; Lavan and Levy 2006; Lin et al. 2014; Tubaldi et al. 2014; Gidaris and Taflanidis 2015; Pollini et al. 2016). They range from approaches utilizing simple schemes, distributing total damping coefficient according to pre-selected simplified criteria, with the total damping coefficient chosen so that a specific performance is achieved, to approaches that establish a formal optimization procedure based on some chosen performance objectives. Simplified approaches adopt a modal analysis philosophy, emphasizing the damping ratio (or transfer function) at the fundamental mode. Other methodologies use time-history analysis and peak response quantities to evaluate structural performance. Between these two extremes in terms of complexity, another wide range of approaches evaluate performance using random vibration theory, modeling the seismic excitation as a stationary stochastic process.

[1]Structural Engineer, Rene Lagos Engineers, Santiago, Chile, fisaitua@uc.cl.
[2]Associate Professor, Pontificia Universidad Católica de Chile & Researcher, National Research Center for Integrated Natural Disaster Management CONICYT FONDAP 15110017, Santiago, Chile, dlg@ing.puc.cl
[3]Associate Professor, University of Notre Dame, Notre Dame, U.S.A, a.taflanidis@nd.edu

Emphasis in the aforementioned studies has been placed on configurations where bracing terminals of the dampers are anchored at consecutive (i.e., adjacent) floor levels. Such an implementation might not be suitable, though, for stiff buildings where interstorey velocities might not be large enough for efficient energy dissipation through supplemental viscous dampers (Baquero Mosquera et al. 2016). This is the case, for example, for Chilean residential buildings where the lateral force resisting system is made up of stiff reinforced concrete members. While studies have shown the efficacy of bracing schemes that amplify the interstorey displacement between adjacent floor levels (Baquero Mosquera et al. 2016), very few researches have considered supplemental dampers attached to braces connecting non-consecutive (i.e., non-adjacent) floor levels. Among researchers that mention this issue, Silvestri and Trombetti (2004) showed that, under the constraint of total supplemental damping (i.e., the sum of the damping coefficients), distributions that include dampers attached to non-consecutive floor levels are more efficient than optimal distributions of dampers attached only to consecutive floor levels, but they did not provide a comprehensive theoretical framework for analysis/design. As such there is a need for a more complete evaluation/comparison of the benefits such a bracing scheme can provide.

This study aims to address this knowledge gap and investigates the optimal height-wise distributions of viscous dampers in multistory structures emphasizing applications for which the dampers are attached to non-consecutive floors. Our intent is to establish a comparison framework appropriate for practical applications. For this purpose unnecessary modeling complexity that might reduce the applicability of the approach is avoided. This is facilitated by modeling structural performance through stationary response statistics. To better illustrate the benefits from the non-consecutive floor damper implementation, performance is quantified in terms of the cost of supplemental dampers. The latter is on its own another relevant contribution of the study. Though the importance of explicitly incorporating the upfront damper cost has been demonstrated in studies relying on advanced numerical modeling of structural behavior (Gidaris and Taflanidis 2015; Pollini et al. 2016), this cost is commonly ignored or is only approximately addressed in simplified design frameworks like the one considered here. In these latter cases usually the total damping coefficient is considered (Singh and Moreschi 2002), but this quantity does not explicitly indicate the damper cost, which is actually more related to the force capacity rather than to the damping coefficient.

In the next section the damper distribution problem formulation is presented, giving special attention to calculation of second order response statistics that will be needed in the design framework latter. Theoretical discussion related to non-consecutive bracing scheme implementation are discussed in Section 3. In Section 4 the cost-based design optimization problem and its solution are discussed. In Section 5 a case study of a real Chilean high-rise building is presented.

2. PROBLEM FORMULATION AND CALCULATION OF RESPONSE STATISTICS

2.1 State-space formulation

Consider a n_s-storey building equipped with n_d viscous dampers (linear or nonlinear) connecting different floor levels as seen in Fig. 1, either with a consecutive (n_c=1) or non-consecutive (n_c>1) bracing scheme. Let $\mathbf{x}_s \in \Re^{n_s}$ be the vector of floor displacements of the primary structure relative to the ground and $\ddot{x}_g \in \Re$ be the ground acceleration. The equation of motion of the structure is given by:

$$\mathbf{M}_s\ddot{\mathbf{x}}_s(t)+\mathbf{C}_s\dot{\mathbf{x}}_s(t)+\mathbf{K}_s\mathbf{x}_s(t)+\mathbf{T}_d^T\mathbf{f}_d(t)=-\mathbf{M}_s\mathbf{R}_s\ddot{x}_g(t)\,, \tag{1}$$

where $\mathbf{M}_s \in \Re^{n_s x n_s}$, $\mathbf{C}_s \in \Re^{n_s x n_s}$, and $\mathbf{K}_s \in \Re^{n_s x n_s}$ are the mass, damping, and stiffness matrices of the primary structure, respectively, $\mathbf{R}_s \in \Re^{n_s}$ is the earthquake influence coefficient vector (vector of ones), $\mathbf{f}_d \in \Re^{n_d}$ is the vector of damper forces and $\mathbf{T}_d \in \Re^{n_d x n_s}$ is the connectivity matrix that relates the velocities of the global degrees of freedom to the vector of relative velocities between the ends of each damper so that $\dot{\mathbf{v}}=\mathbf{T}_d\dot{\mathbf{x}}_s$, where $\dot{\mathbf{v}}$ stands for the damper relative velocities. Let $\ddot{x}_g$ be modeled as a stationary filtered Gaussian white noise stochastic process. A state-space formulation is utilized to determine the response statistics. In this setting, the excitation model is

$$\dot{\mathbf{x}}_q(t) = \mathbf{A}_q \mathbf{x}_q(t) + \mathbf{E}_q w(t); \quad \ddot{x}_g(t) = \mathbf{C}_q \mathbf{x}_q(t), \tag{2}$$

where $w(t) \in \Re$ is a zero-mean Gaussian white-noise process with spectral intensity equal to $S_w = 1/(2\pi)$; $\mathbf{x}_q(t) \in \Re^{n_q}$ is the state vector for the excitation; $\mathbf{A}_q \in \Re^{n_q \times n_q}$, $\mathbf{E}_q \in \Re^{n_q \times 1}$ and $\mathbf{C}_q \in \Re^{1 \times n_q}$ are the state-space excitation matrices. Combining excitation model of Equation (2) with the equations of motion of the structural system (1) provides the augmented state-space system

$$\dot{\mathbf{x}}(t) = \mathbf{A}\mathbf{x}(t) + \mathbf{B}\mathbf{f}_d(t) + \mathbf{E}w(t); \quad \mathbf{z}(t) = \mathbf{C}\mathbf{x}(t) + \mathbf{D}\mathbf{f}_d(t), \tag{3}$$

where $\mathbf{x}(t) \in \Re^{n_x}$ is the state vector with $n_x = 2n_s + n_q$; $\mathbf{z}(t) \in \Re^{n_z}$ is the vector of performance variables (response output of the system) with z_i denoting the i^{th} output; and **A**, **B, E**, **C, D** are the system state-space matrices. Note that the proposed formulation takes into account the spectral characteristics of the stochastic excitation, by appropriate augmentation of the state equation (Taflanidis and Scruggs 2010). The derivation of the state space matrices is discussed in the Appendix.

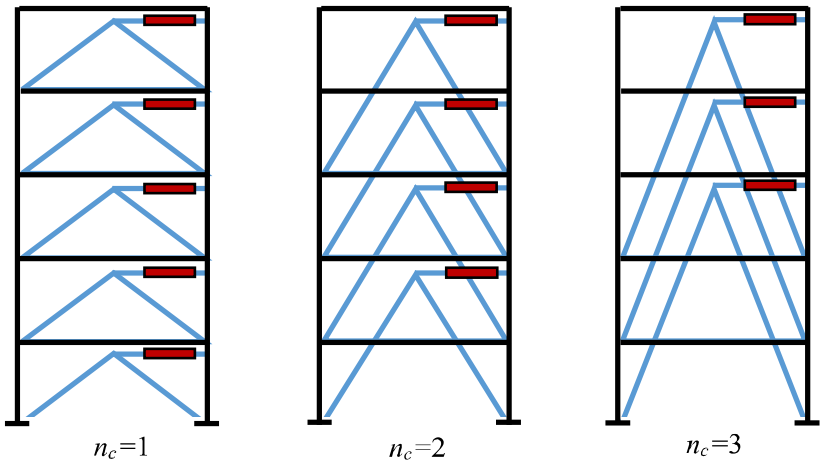

Figure 1. Multistorey structure with dampers using different connectivity schemes

The force demand on the i-th viscous damper of the system is given by $f_{di} = c_{di} |\dot{v}_i|^{\alpha_i} \text{sgn}(\dot{v}_i)$ where α_i, c_{di} and $\dot{v}_i$ are the viscous exponent, damping coefficient and relative velocity of the i-th viscous damper, and sgn(.) is the signum function. For linear dampers α_i=1 whereas for nonlinear dampers statistical linearization can be employed to replace the nonlinear force with an equivalent linear one. In this case, the equivalent damping coefficient of the i-th viscous damper c_{eqi} is given by (Di Paola and Navarra 2009):

$$c_{eqi} = c_{di} \frac{2^{1+\frac{\alpha_i}{2}} \Gamma(1+\frac{\alpha_i}{2})}{\sqrt{2\pi}} \sigma_{\dot{v}i}^{\alpha_i - 1} \tag{4}$$

where $\Gamma(.)$ is the Gamma function and $\sigma_{\dot{v}i}$ is the standard deviation of $\dot{v}_i$. The linearized damper force is then $f_{di} = c_{eqi}\dot{v}_i$. The damper force vector $\mathbf{f}_d$, with elements f_{di}, can be expressed as $\mathbf{f}_d = \mathbf{K}(\mathbf{c}_{eq})\dot{\mathbf{v}}$ where $\mathbf{K}(\mathbf{c}_{eq})$ is a diagonal matrix with the equivalent damping coefficient c_{eqi} of each damper. Relative velocities are given by $\dot{\mathbf{v}} = \mathbf{T}_d \dot{\mathbf{x}}_s = \mathbf{L}_d \mathbf{x}$, where $\mathbf{L}_d$ is the state connectivity matrix that relates these velocities to the state vector, also given in the Appendix, and the dependence of $\mathbf{K}$ on $\mathbf{c}_{eq}$ is explicitly emphasized. We can finally formulate the final state-space system representation

$$\begin{aligned} &\dot{\mathbf{x}}(t) = \mathbf{A}_a(\mathbf{c}_{eq})\mathbf{x}(t) + \mathbf{E}w(t); \quad \mathbf{z}(t) = \mathbf{C}_a(\mathbf{c}_{eq})\mathbf{x}(t) \\ &\text{where } \mathbf{A}_a(\mathbf{c}_{eq}) = \mathbf{A} + \mathbf{B}\mathbf{K}(\mathbf{c}_{eq})\mathbf{L}_d; \; \mathbf{C}_a(\mathbf{c}_{eq}) = \mathbf{C} + \mathbf{D}\mathbf{K}(\mathbf{c}_{eq})\mathbf{L}_d. \end{aligned} \tag{5}$$

2.2 Response statistics estimation

Under the modelling assumptions discussed above, the output of the system, $\mathbf{z}(t)$, has a Gaussian distribution with zero mean and covariance matrix in stationary response given as

$$\mathbf{K_{zz}} = \mathbf{C}_a(\mathbf{c}_{eq})\mathbf{P}(\mathbf{c}_{eq})\mathbf{C}_a(\mathbf{c}_{eq})^T;\ \mathbf{A}_a(\mathbf{c}_{eq})\mathbf{P}(\mathbf{c}_{eq}) + \mathbf{P}(\mathbf{c}_{eq})\mathbf{A}_a(\mathbf{c}_{eq})^T + \mathbf{E}\mathbf{E}^{\mathrm{T}} = 0\,, \tag{6}$$

where $\mathbf{P}(\mathbf{c}_{eq})$ corresponds to the state covariance matrix, obtained, as shown above, by the solution of an algebraic Lyapunov equation (Lutes and Sarkani 1997). The variance of each of the n_z system output variables is given by the corresponding element of the diagonal of $\mathbf{K}_{zz}$. The variances of the damper relative velocities are also needed in the problem formulation and are related to the state covariance matrix by:

$$\boldsymbol{\sigma}^2_{\dot{\mathbf{v}}} = \mathbf{L}_d^T\mathbf{P}(\mathbf{c}_{eq})\mathbf{L}_d\,. \tag{7}$$

Using these variances, the RMS damper forces can be obtained as:

$$\boldsymbol{\sigma}_{\mathbf{f}_d} = \mathbf{K}(\mathbf{c}_{eq})\boldsymbol{\sigma}_{\dot{\mathbf{v}}}\,. \tag{8}$$

When statistical linearization is employed, variances $\boldsymbol{\sigma}^2_{\dot{\mathbf{v}}}$ are also used to calculate the equivalent damping coefficient given by Equation (4). In this case a cyclic dependence exists: c_{eqi} depends on $\sigma_{\dot{v}i}$ based on Equation (4), but based on Equation (7) and the dependence on $\mathbf{P}(\mathbf{c}_{eq})$, the latter also depends (implicitly) on c_{eqi}. An iterative process is therefore needed to solve for the equivalent damper coefficients and the state covariance matrix. In the context of the optimization established later in this study this is avoided by adopting the equivalent damping coefficients as the primary design variables, and then back-deriving the actual damping coefficients. In this case there is no iterative process required. Once c_{eqi} is known, $\sigma_{\dot{v}i}$ can be solved for by calculating the second order statistics, and finally c_{di} can be computed using Equation (4).

3. THEORETICAL ASSESSMENT OF NON-CONSECUTIVE BRACING SCHEMES

To theoretically demonstrate the advantages of the n_c>1 approach, we will examine a simplified analytical comparison. We will consider here the case of a single damper, although the philosophy underlying this reasoning can extend directly to systems equipped with multiple dampers. To provide greater clarity in the discussion we will focus on harmonic excitation with frequency ω. Denoting the amplitude of the relative displacement between the ends of the damper as v_o, the energy dissipated E_d by a single damper is given by (Symans and Constantinou 1998):

$$E_d = c_d\omega^\alpha v_o^{1+\alpha}2^{\alpha+2}\Gamma^2\left(1+\frac{\alpha}{2}\right)/\Gamma(2+\alpha) = c_d\omega^\alpha v_o^{1+\alpha}g(\alpha);\quad g(\alpha) = 2^{\alpha+2}\Gamma^2\left(1+\frac{\alpha}{2}\right)/\Gamma(2+\alpha)\,, \tag{9}$$

where α denotes the viscous exponent and c_d the damping coefficient. Assuming that lateral displacements varies linearly with height and that axial deformations of the dampers are linearly related to interstorey deformations, the peak deformation of the damper v_{on_c} when the bracing scheme is such that n_c>1 is $v_{on_c} = n_c v_{o1}$, where v_{o1} is the peak damper deformation for n_c=1. Same energy dissipation capability is needed to achieve the same level of vibration suppression independent of the value of n_c (this can be viewed as equivalent to establishing the same improvement in damping ratio). Therefore, for a given performance level, when n_c>1 the viscous damper coefficient c_{dn_c} must satisfy:

$$E_{d1} = E_{dn_c} \rightarrow c_{d1}\omega^\alpha v_{o1}^{1+\alpha}g(\alpha) = c_{dn_c}\omega^\alpha\left(n_c v_{o1}\right)^{1+\alpha}g(\alpha) \rightarrow c_{dn_c} = \frac{c_{d1}}{n_c^{1+\alpha}}\,, \tag{10}$$

This result shows that, if the energy dissipation (and therefore performance) is fixed, a n_c>1 bracing scheme leads to a total damping coefficient that is $n_c^{1+\alpha}$ times smaller than the total damping coefficient of the n_c=1 bracing scheme. Alternatively, Equation (10) indicates that for a given total damping coefficient the energy dissipated by a n_c>1 bracing scheme is $n_c^{1+\alpha}$ times higher than the energy dissipated by the n_c=1 bracing scheme.

By itself, the value of the damping coefficient is not of significant practical interest because, as mentioned in the introduction, it has no direct relationship to the damper cost. In fact, the relevant quantity related to cost estimation is the force capacity of the damper, which obviously must be greater than the force demand on the damper. Based on the assumption that lateral displacements varies linearly with height, so do velocities under harmonic excitation of the same frequency. Therefore, when n_c>1 the relative velocity between damper terminals is approximately n_c times greater than the relative velocity when n_c=1. This leads to relationship for forces:

$$f_{dn_c} = c_{dn_c}\left|\dot{v}_{n_c}\right|^{\alpha} = \frac{c_{d1}}{n_c^{1+\alpha}}\left|n_c\dot{v}_1\right|^{\alpha} = \frac{1}{n_c}c_{d1}\left|\dot{v}_1\right|^{\alpha} = \frac{f_{d1}}{n_c}, \tag{11}$$

which means that, with respect to the case where n_c=1, damper forces are reduced by a factor of n_c regardless of the value of α. Since damper forces are directly related to damper cost, this result shows that n_c>1 bracing schemes might induce a significant reduction of damper cost. To further investigate this trends a height-wise damper distribution optimization scheme that explicitly considers cost associated with damper forces is examined next.

4. COST BASED OPTIMAL DAMPER DISTRIBUTION

The design objective is to identify the optimal damping coefficient vector $\mathbf{c}_d$ made up of the damper coefficients of all supplemental dampers. To simplify the optimization, the equivalent damping coefficient is posed as the design optimization vector as discussed earlier, and then Equation (4) is applied to determine $\mathbf{c}_d$ (note that if dampers are linear, $\mathbf{c}_d$=$\mathbf{c}_{eq}$). Design objectives are related to the cost of implementation of the supplemental damping system whereas considerations about the established vibration suppression level are incorporated through performance constraints.

4.1 Cost-based objective functions

Two different cost functions are considered. The first and simplest one is the sum of RMS damper forces, i.e.:

$$J_1(\mathbf{c}_{eq}) = \sum_{i=1}^{n_d}\sigma_{f_d i}, \tag{12}$$

where $\sigma_{f_d i}$ is the RMS force demand on the i-th damper, given by components of vector in Equaiton (8), and J_1 has units of force. This measure facilitates a closer connection to the damper cost (Gidaris and Taflanidis 2015) than the commonly adopted (Singh and Moreschi 2002) total damping coefficient C_o (sum of each damping coefficient c_{di}). However, damper cost is actually related to damper force capacity, which is a function of the *peak* damper force rather than of the RMS response. Moreover, this cost is not linearly related to damper force capacity (Gidaris and Taflanidis 2015). The second cost function incorporates these considerations, and is given by:

$$J_2(\mathbf{c}_{eq}) = 96.88\sum_{i=1}^{n_d} f_{doi}^{0.607}, \tag{13}$$

where f_{doi} is the *peak* force demand on the i-th damper (in units of kN) and J_2 is expressed in United States Dollars (USD). For linear dampers peak force quantities can be approximately related to RMS values as $f_{doi} = p_f\sigma_{f_d i}$, where p_f is the peak factor, relating the mean of the peak damper force (or peak

of any stochastic variable) to its standard deviation. In this study this factor is taken as 2, corresponding to a single degree of freedom oscillator with 5% damping vibrating for 20 cycles based on up-crossing rate (Der Kiureghian 1980), the latter representing the period of vibration for stochastic variables. The 20 cycles were chosen to accommodate the case study considered later, based on strong ground motion duration characteristics for the region and the fundamental period of the building structure. For nonlinear dampers a modification is warranted since accuracy of statistical linearization typically reduces for peak response quantities, compared to the accuracy of average/RMS response quantities (Roberts and Spanos 2003). Since intent of developed framework is to have practical utility, a simplified approximation is adopted to estimate peak damper forces. These are assumed equal to the forces developed for a specific peak velocity, and therefore are given by:

$$f_{doi} = c_{di}(p_f \sigma_{\dot{v}i})^{\alpha} . \tag{14}$$

The relationship in Equation (13) between the damper force capacity and the damper cost was derived from the analysis of available commercial information (Gidaris and Taflanidis 2015) and indicates that the cost of a marginal increment in force capacity is smaller in dampers having a large force capacity than in dampers having a small force capacity. This cost function, though, does not incorporate considerations about the maximum feasible damper force capacity $f_{\max}$ of commercially available dampers. Of course larger values of f_{doi} can be accommodated by using multiple dampers per storey, with the capacities of each damper limited to $f_{\max}$. In this case, though, the cost per damper is related to each individual force capacity and not the total capacity per storey. To address this issue, the following modification, is proposed, assuming that if at some storey f_{doi} exceeds $f_{\max}$ then such demand will be accommodated using multiple, equal capacity dampers, the number of which is the smallest number needed so that the force capacity of each damper is smaller than $f_{\max}$

$$J_{2m}(\mathbf{c}_{eq}) = 96.88 \sum_{i=1}^{n_d} \left[\frac{f_{doi}}{f_{\max}} \right] \left(f_{doi} \Big/ \left[\frac{f_{doi}}{f_{\max}} \right] \right)^{0.607} , \tag{15}$$

where [.] is the ceiling function.

4.2 Functions related to structural performance

The function incorporating structural performance considerations in the design can be described based on second order statistics of the output. Since seismic performance is typically expressed in terms of occurrence of different failure modes, quantified by engineering demand parameters exceeding certain thresholds, it is reasonable to define performance in terms of the maximum normalized variance. The latter is directly related to the probability of occurrence of any failure mode in the structure (Taflanidis and Scruggs 2010). This approach leads to definition for the performance function as $h(\boldsymbol{\sigma}_z) = \max_k(\lambda_k \sigma_{zk} / \beta_k)$, where λ_k and β_k are the relative importance and normalization constant of the k-th output of $\mathbf{z}$, respectively.

4.3 Height-wise optimal distribution design problem

The optimization problem is formulated as constrained optimization with cost metric J_l [where l refers to different alternatives, J_1 or J_2/J_{2m}] corresponding to the objective function to be minimized and the performance function $h(\boldsymbol{\sigma}_z)$ corresponding to the constraint. At the design stage focus is placed on the interstorey drift performance, leading to λ_k=0 for performance outputs associated with accelerations and λ_k=1 or the outputs associated with the interstorey drifts. Threshold β_k is chosen same for all drifts and equal to the maximum RMS interstorey drift response of the structure without dampers. This constraint selection ultimately facilitates the identification of the damper distribution providing a target reduction of the interstorey drift response with respect to that of the uncontrolled structure. The optimization problem is expressed as:

$$\mathbf{c}_{eq}{}^{*} = \arg\min_{\mathbf{c}_{eq} \in \Re_{+}^{n_d}} J_1(\mathbf{c_{eq}}) \text{ such that } \frac{\max_j \left[\sigma_{\delta j}(\mathbf{c}_{eq}) \right]}{\overline{\sigma_{\delta o}}} \le c_{tg} \,, \tag{16}$$

where $\sigma_{\delta j}$ is the RMS interstorey drift response at the j-th storey of the structure equipped with dampers and c_{tg} is the target performance (vibration suppression ratio with respect to the uncontrolled structure). This optimization problem corresponds to a nonlinear constrained optimization problem with potentially multiple local minima (non-convex characteristics). The challenges in this optimization problem stem from multiple sources: nonlinearities in the objective functions and constraints (use of max function for the latter creates a non-smooth problem), and trade-off in the performance between the capacity of dampers at different floors. To address these challenges a global optimization algorithm is adopted and implemented through the TOMLAB optimization environment (Holmstrom et al. 2009).

Should be pointed out that in the case of nonlinear dampers, cost function J_1 does not change in the sense that linear and nonlinear damper distributions having the same values of c_{eqi} (equal to c_{di} for linear dampers) lead to the same value of J_1. The J_2 (or J_{2m}) objective function, though, does take different values depending on whether dampers are a linear or nonlinear. The difference stems from the modification established to calculate the peak damper force given by Equation (14). If this modification was not established, and peak forces were calculated using direct statistical linearization, no differences would exist.

5. CASE STUDY

The design framework is illustrated next for the retrofit of an existing 26-storey Chilean building (Ugalde and Lopez-Garcia 2017) with viscous dampers. The chosen building, having base dimensions of 18 by 23 meters, total seismic weight of 11690 tonf and typical storey-height of 2.52 meters, is a typical example of Chilean high-rise building (in terms of structural properties and modal characteristics). Three different design cases are examined with respect to the objective function definition, J_1, J_2 or J_{2m} and will be referenced, respectively, as D_1, D_2 and D_{2m}. The target reduction of interstorey drift response is set equal to 40% i.e., c_{tg} chosen as 0.60. Based on commercially available data maximum force capacity $f_{\max}$ of a single damper is set equal to 815 tonf. Note that tonf is used herein to describe forces, as is the standard in the Chilean region. Conversion to kN, if desired, can be established by multiplying given force values by g constant.

5.1 Structural and excitation models

Two 2D models are developed for the structure (one along each of the two main orthogonal axes x and y), obtained by static condensation of the initial 3D structural model. The degrees of freedom of the resulting 2D models are the lateral floor displacements of each of the 26 storeys. The 2D models are denoted 26X and 26Y, respectively, and their first and second vibration periods are 1.29 sec, 0.30 sec, in the x direction and 1.51 sec, 0.35 sec, in the y direction. The modal participating mass ratios of the first and second mode are 0.69 and 0.18 for the 26X model, and 0.66 and 0.18 for the 26Y model. The inherent damping is assumed equal to 5% for all modes.

The stationary seismic excitation $\ddot{x}_g$ is described by a high-pass filtered Kanai-Tajimi power spectrum (Clough and Penzien 1993)

$$S_g(\omega) = s_o \frac{\omega_g^4 + 4\zeta_g^2 \omega^2 \omega_g^2}{\left(\omega_g^2 - \omega^2\right)^2 + 4\zeta_g^2 \omega_g^2 \omega^2} \frac{\omega^4}{\left(\omega_f^2 - \omega^2\right)^2 + 4\zeta_f^2 \omega_f^2 \omega^2} \,. \tag{17}$$

In the above equation parameters ω_g and ζ_g represent the stiffness/frequency and damping properties,

respectively, of the supporting ground modeled by a linear damped SDOF oscillator driven by white noise. Further, parameters ω_f and ζ_f control the cut-off frequency and the "steepness" of a high-pass filter used to suppress the low frequency content allowed by the Kanai-Tajimi filter. Lastly, s_o is chosen to achieve a desired value for the root mean square acceleration a_{RMS} of the considered seismic input. The parameters of the filter are chosen through calibration to a suite of ground motions that are representative of the Chilean seismic hazard. Ground motions recorded during the M_w 8.8 2010 Maule (Chile) earthquake are chosen for this purpose. From the available ground motions, only the ones recorded on what is defined as Soil Type II (soft rock or stiff soil) in the Chilean seismic design code NCh433 are considered. Soil Type II is the soil type at the location of the considered building. This calibration leads to values ω_g=16.46 rad/s, ζ_g=0.6, ω_f=6.845 rad/s, ζ_f=0.48. a_{RMS} is calculated based on a target Peak Ground Acceleration (PGA), with the latter defined based on NCh433 provisions for Seismic Zone 2 (where Santiago City is located) as 0.30g. Assuming a peak factor of 2 (same value adopted earlier), the target a_{RMS} is then 0.15g.

5.2 Results and discussion

The height-wise optimization is performed for linear dampers (α=1) for both models 26X and 26Y and for nonlinear dampers with α=0.35 for model 26X. Latter case will be references with superscript *nl* herein. To investigate the benefits of the height-wise damper distributions given by the proposed explicit optimization approach, two other well-known height-wise distribution schemes are considered here. The first approach is the Uniform distribution, i.e., same damper capacity in all storeys. The second approach is the Sequential Search Algorithm SSA (Zhang and Soong 1992), where dampers are placed sequentially at the storey where the value of a performance index (interstorey drift in this study) reaches a maximum. The computation of the performance index is based on the second order statistics of the response. In both schemes the same target performance is adopted, i.e. reduction of drift corresponding to c_{tg}. The superscripts *U* and *SSA* are used, respectively, to describe these two simplified distributions.

Results for n_c=1 are presented in Table 1 and Fig. 2. Table 1 presents: all cost functions J_l evaluated at optimal design vector for each design case; maximum peak force over all dampers max(f_{do}); damping ratio of the retrofitted structure at the fundamental mode ξ; mean ratio per storey of RMS interstorey drifts $\overline{\sigma_\delta / \sigma_{\delta o}}$ and floor accelerations $\overline{\sigma_a / \sigma_{ao}}$ with respect to the RMS values of the structure without dampers, which is a representation of the average response reduction per storey; the cost reduction J_l / J_l^U and J_l / J_l^{SSA} with respect to the *U* and *SSA* distributions offered by the explicit height-wise optimization scheme; the cost reduction J_l^{nl} / J_l for the nonlinear damper implementation. For the last three quantities performance is reported for each design with respect to the corresponding cost function used in the optimization, for example when design case D_1 is examined the ratio of objective functions J_l / J_l^{SSA} corresponds to cost function J_1 (l=1). The height-wise distribution of the peak-damper forces is shown in Fig 2 for model 26X.

Table 1: Response quantities of interest for models 26X and 26Y for different design cases (n_c=1).

Case		Linear dampers									Comparison to nonlinear $\frac{J_l^{nl}}{J_l}$
		J_1 [tonf]	J_2 [10^3 USD]	J_{2m} [10^3 USD]	max(f_{do}) [tonf]	ξ [%]	$\overline{\sigma_\delta / \sigma_{\delta o}}$ [%]	$\overline{\sigma_a / \sigma_{ao}}$ [%]	$\frac{J_l}{J_l^U}$	$\frac{J_l}{J_l^{SSA}}$	
26x	D_1	2553	161	187	1382	14.3	59	55	0.90	0.93	1
	D_2	2829	90	165	4775	15.9	60	62	0.34	0.69	0.84
	D_{2m}	2601	117	159	2256	14.4	60	56	0.40	0.89	0.84
26y	D_1	2126	97	142	1706	14.2	61	55	0.88	0.96	n/a
	D_2	2447	79	144	4458	17.0	61	60	0.33	0.73	
	D_{2m}	2195	84	131	3262	15	61	57	0.61	0.95	

Results show that design case D_1 minimizes force demands on dampers but at the expense of relatively

large values of cost-related objectives J_2 and J_{2m}. D_2 design leads to reductions in J_2 equal to 44% in model 26X and 18% in model 26Y, although at the expense of large values of maximum peak damper force that might not be feasible. The maximum damper force max(f_{do}) exceeds the feasible limit of 815 tonf for a single damper. This means that design case D_{2m} is different from its counterpart that does not explicitly incorporate maximum force capacity considerations. Results indicate that consideration of f_{max} leads to designs having not only smaller values of J_{2m} (as expected) but also smaller values of max(f_{do}). This shows that consideration of the maximum force in the damper cost leads to a distribution that avoids excessively large dampers placed at a single storey. This is also evident in Fig 2 results. Moreover, for D_{2m} design mean floor acceleration reduction per storey seems to be reduced up to 6% more with respect to is counterpart (D_2), which is another advantage of the more uniform distribution established through considering the maximum force capacity. With respect to the overall damper efficiency the results show that similar vibration suppression is established through all design cases, with the targeted reduction of 40% for maximum interstorey drift established with approximately 10% of supplemental damping ratio (as intrinsic damping ratio is 5%). Such a supplemental damping threshold has been set as a reasonable objective in many viscous damper applications. With respect to the interstorey drift and floor acceleration reduction, the mean drift reduction per storey $\sigma_\delta / \sigma_{\delta o}$ and mean acceleration reduction per storey σ_a / σ_{ao} take similar values as the target of 40% reduction of the maximum drift. This shows that the proposed design scheme establishes a similar vibration suppression across all storeys, not only at the storeys where interstory drifts are maximized.

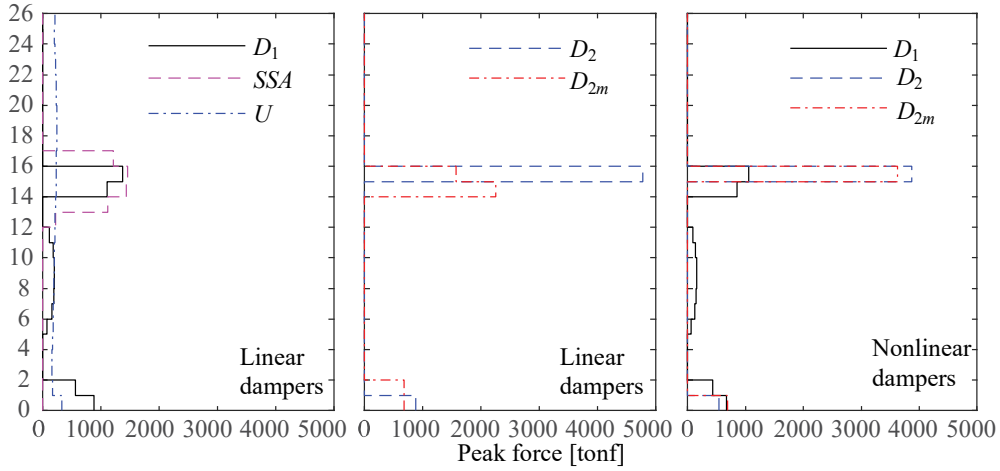

Figure 2. Distribution of peak damper forces for different implementations for n_c=1 and model 26X

Comparison to simplified distribution schemes clearly indicates that the proposed explicit design approach leads to noticeably benefits. Differences are more noticeable when nonlinearities in the target cost function are more relevant and no constraints exist for maximum damper forces (so scheme is allowed to benefit more from an imbalanced distribution), i.e. bigger differences in the D_2 design case rather than D_{2m}. While cost is not explicitly considered in its formulation, *SSA* is generally more cost-effective than *U* distribution, most likely because, albeit simplified and sequential in nature (rather than targeting total optimality), still incorporates an explicit damper distribution based on optimality criteria and structural performance. Comparison between linear and nonlinear implementations indicates that, for a given level of structural performance, nonlinear dampers are more cost effective. Note that, as mentioned in Section 4 the value of the J_1 metric is independent of whether the dampers are linear or nonlinear (optimal distribution with respect to equivalent viscous damping is the same), which is why J_1^{nl} / J_1 ratio is equal to unity.

Results for n_c>1 are presented in Table 2, and Fig. 3, focusing on the performance improvement between n_c>1 and n_c=1 cases. To facilitate an easier presentation herein subscript "1" refers to the case where n_c=1 and subscript "n_c" indicates the case where n_c>1. Results reported Table 2 focus on comparison between n_c=1 and n_c>1 cases: fundamental mode damping ratio ξ_1 / ξ_{n_c}; total damping

coefficient ratio C_{o1}/C_{on_c}; RMS damper velocities ratio $\overline{\sigma_{\dot{v}1}}/\overline{\sigma_{\dot{v}n_c}}$; ratio of objectives J_{l1}/J_{ln_c}. Additionally the performance improvement compared to the *SSA* distribution J_l/J_l^{SSA} for each n_c value is also shown. Results clearly indicate that, for the same level of energy dissipation, when n_c>1 the value of all cost functions is reduced by a factor approximately equal to n_c with respect to that when n_c=1. The fundamental mode damping ratio (representative of energy dissipation) remains essentially constant (i.e., $\xi_1/\xi_{n_c}\approx 1$), but the sum of damper coefficients C_o is reduced by a factor roughly equal to $n_c^{1+a}=n_c^2$ for linear dampers (4 and 9 for n_c=2 and 4, respectively) and $n_c^{1+a}=n_c^{1.35}$ for nonlinear dampers, (2.55 and 4.41 for n_c=2 and 4, respectively), while damper velocities $\sigma_{\dot{v}}$ increase by a factor roughly equal to n_c, which leads to an average decrease of damper forces (and consequently of costs) by a factor approximately equal to n_c. These results are consistent with the theoretical discussion in Section 3 and highlight under realistic application and modeling assumptions the benefits of bracing schemes where supplemental dampers are anchored at non-consecutive floor levels.

Table 2: Effect of n_c on different response quantities of interest

Case			n_c=2					n_c=3				
			ξ_1/ξ_{n_c}	C_{o1}/C_{on_c}	$\overline{\sigma_{\dot{v}1}}/\overline{\sigma_{\dot{v}n_c}}$	J_{l1}/J_{ln_c}	J_l/J_l^{SSA}	ξ_1/ξ_{n_c}	C_{o1}/C_{on_c}	$\overline{\sigma_{\dot{v}1}}/\overline{\sigma_{\dot{v}n_c}}$	J_{l1}/J_{ln_c}	J_l/J_l^{SSA}
26x	*linear*	D_1	1	3.95	2.01	1.98	0.93	1	8.68	3.03	2.91	0.96
		D_2	0.96	4.17	2.19	1.89	0.70	1.02	7.51	2.70	2.98	0.93
		D_{2m}	0.85	2.78	1.83	1.64	0.86	0.95	9.00	3.34	2.80	0.92
	α=0.35		1.06	2.83	1.98	2.02	n/a	1.01	4.21	2.89	3.36	n/a
26y	*linear*	D_1	0.98	4.41	2.22	1.95	0.98	0.97	9.71	3.31	2.89	0.98
		D_2	1.06	4.68	2.09	2.09	0.59	1.12	10.71	2.84	3.14	0.66
		D_{2m}	1.04	4.33	1.99	2.15	0.83	1.00	8.39	2.76	2.94	0.88

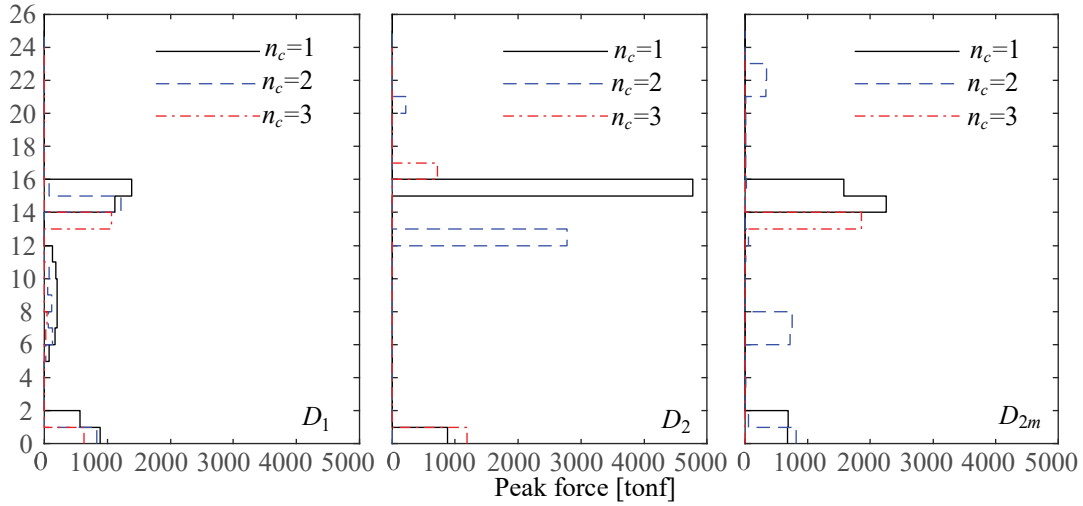

Figure 3. Distribution of peak damper forces for linear damper implementations for model 26X

6. CONCLUSSIONS

The cost-based optimal height-wise distributions of viscous dampers in multistory structures was investigated in this paper emphasizing applications for which the dampers are attached to non-consecutive floors. Seismic excitation was modeled as a stochastic process, and response statistics were obtained through state-space analysis. Different cost functions that account (with different sophistication levels) for different relationships between cost and damper force capacity and maximum feasible damper force capacity were considered. The performance function was defined in terms of the interstorey drift response, and was used as a constraint function by imposing a target reduction of the response in comparison to the uncontrolled structure. As case study application to a 26-storey Chilean

high-rise reinforced concrete building was examined. Results indicate that the explicit optimization of the damper distribution considering realistic cost metrics leads to significant savings with respect to damper distributions optimized for simplified cost metrics. Consideration of feasible damper maximum force capacity also has a significant influence on the optimal damper distribution. More importantly, bracing schemes with dampers connected every n_c floor levels (n_c>1) reduce damper force demand by factor approximately equal to n_c for the same protection level, something that can contribute to significant cost savings. This was validated both using simplified assumptions (harmonic response) as well as under more realistic modeling and for both linear and nonlinear dampers. For nonlinear dampers it was shown, in general, that explicit consideration of nonlinearities for peak response calculation produces results that can be more cost-effective.

7. ACKNOWLEDGMENTS

Financial support was provided by the National Research Center for Integrated Natural Disaster Management CONICYT FONDAP 15110017 (Santiago, Chile) and by CONICYT through the programs CONICYT-PCHA/MagisterNacional/2016-22161043 and Beca Ciencia y Tecnologia, Estadias Cortas 2015. The dynamic properties of the structure considered in the case study described in Section 5 were provided by VMB Ingenieria Estructural (Santiago, Chile).

8. REFERENCES

Baquero Mosquera, J. S., Almazán, J. L., and Tapia, N. F. (2016). "Amplification system for concentrated and distributed energy dissipation devices." *Earthquake Engineering & Structural Dynamics*, 45(6), 935-956.

Clough, R. W., and Penzien, J. (1993). *Dynamics of structures*, McGraw-Hill Inc., New York, N.Y.

Der Kiureghian, A. (1980). "Structural response to stationary excitation." *Journal of Engineering Mechanics, ASCE*, 106((EM6)), 1195-1213.

Di Paola, M., and Navarra, G. (2009). "Stochastic seismic analysis of MDOF structures with nonlinear viscous dampers." *Structural Control and Health Monitoring*, 16(3), 303-318.

Gidaris, I., and Taflanidis, A. A. (2015). "Performance assessment and optimization of fluid viscous dampers through life-cycle cost criteria and comparison to alternative design approaches." *Bulletin of Earthquake Engineering*, 13(4), 1003-1028.

Holmstrom, K., Goran, A. O., and Edvall, M. M. (2009). *User's guide for TOMLAB 7*, Tomlab Optimization Inc. www.tomopt.com/tomlab/, San Diego, CA.

Lavan, O., and Levy, R. (2006). "Optimal design of supplemental viscous dampers for linear framed structures." *Earthquake engineering & structural dynamics*, 35(3), 337-356.

Lin, J.-L., Bui, M.-T., and Tsai, K.-C. (2014). "An energy-based approach to the generalized optimal locations of viscous dampers in two-way asymmetrical buildings." *Earthquake Spectra*, 30(2), 867-889.

Lopez-Garcia, D. (2001). "A simple method for the design of optimal damper configurations in MDOF structures." *Earthquake Spectra*, 17(3), 387-398.

Lutes, L. D., and Sarkani, S. (1997). *Stochastic analysis of structural and mechanical vibrations*, Prentice Hall, Upper Saddle River, NJ.

Pollini, N., Lavan, O., and Amir, O. (2016). "Towards realistic minimum-cost optimization of viscous fluid dampers for seismic retrofitting." *Bulletin of Earthquake Engineering*, 14(3), 971-998.

Roberts, J. B., and Spanos, P. D. (2003). *Random vibration and statistical linearization*, Dover, Mineola, NY.

Silvestri, S., and Trombetti, T. (2004)."Optimal insertion of viscous dampers into shear-type structures: dissipative properties of the MPD system." *Proceedings of the 13th World Conference on Earthquake Engineering*, 1-6.

Singh, M. P., and Moreschi, L. M. (2002). "Optimal placement of dampers for passive response control." *Earthquake Engineering & Structural Dynamics*, 31(4), 955-976.

Symans, M., and Constantinou, M. (1998). "Passive fluid viscous damping systems for seismic energy dissipation." *ISET Journal of Earthquake Technology*, 35(4), 185-206.

Symans, M. D., Charney, F. A., Whittaker, A. S., Constantinou, M. C., Kircher, C. A., Johnson, M. W., and McNamara, R. J. (2008). "Energy Dissipation Systems for Seismic Applications: Current Practice and Recent Developments." *Journal of Structural Engineering*, 134(1), 3-21.

Taflanidis, A. A., and Scruggs, J. T. (2010). "Performance measures and optimal design of linear structural systems under stochastic stationary excitation." *Structural Safety*, 32(5), 305-315.

Takewaki, I. (1997). "Optimal damper placement for minimum transfer functions." *Earthquake Engineering & Structural Dynamics*, 26(11), 1113-1124.

Tubaldi, E., Barbato, M., and Dall'Asta, A. (2014). "Performance-based seismic risk assessment for buildings equipped with linear and nonlinear viscous dampers." *Engineering Structures*, 78, 90-99.

Ugalde, D., and Lopez-Garcia, D. (2017)."Elastic Overstrength of Reinforced Concrete Shear Wall Buildings in Chile." *16th World Conference on Earthquake Engineering*.

Whittle, J., Williams, M., Karavasilis, T. L., and Blakeborough, A. (2012). "A comparison of viscous damper placement methods for improving seismic building design." *Journal of Earthquake Engineering*, 16(4), 540-560.

Zhang, R.-H., and Soong, T. (1992). "Seismic design of viscoelastic dampers for structural applications." *Journal of Structural Engineering*, 118(5), 1375-1392.

APPENDIX

The state-space representation of the structure in Equation (1) is

$$\dot{\mathbf{x}}_{ss}(t) = \mathbf{A}_s \mathbf{x}_{ss}(t) + \mathbf{B}_s \mathbf{f}_d(t) + \mathbf{E}_s \ddot{x}_g(t), \qquad \mathbf{z}(t) = \mathbf{C}_s \mathbf{x}_{ss}(t) + \mathbf{D}_s \mathbf{f}_d(t) \tag{18}$$

where $\mathbf{x}_{ss} \in \Re^{2n}$ is the state vector collecting relative to the ground displacements and velocities of all stories $\mathbf{x}_{ss} = [\mathbf{x}_s^T \quad \dot{\mathbf{x}}_s^T]^T$, and the matrices in Equation (18) are defined as

$$\mathbf{A}_s = \begin{bmatrix} \mathbf{0}_{n_s x n_s} & \mathbf{I}_{n_s} \\ -\mathbf{M}_s^{-1}\mathbf{K}_s & -\mathbf{M}_s^{-1}\mathbf{C}_s \end{bmatrix} \quad \mathbf{B}_s = \begin{bmatrix} \mathbf{0}_{n_s x n_d} \\ -\mathbf{T}_d^T \end{bmatrix} \quad \mathbf{E}_s = \begin{bmatrix} \mathbf{0}_{n_s x 1} \\ -\mathbf{R}_s \end{bmatrix} \quad \mathbf{C}_s = \begin{bmatrix} \mathbf{T}_s & \mathbf{0}_{n_s x n_s} \\ -\mathbf{M}_s^{-1}\mathbf{K}_s & -\mathbf{M}_s^{-1}\mathbf{C}_s \end{bmatrix} \quad \mathbf{D}_s = \begin{bmatrix} \mathbf{0}_{n_s x n_d} \\ -\mathbf{M}_s^{-1}\mathbf{T}_d^T \end{bmatrix} \tag{19}$$

In the above expressions, the output matrix $\mathbf{C}_s$ accounts for output variables vector **z** that includes inter-storey drifts and absolute accelerations for all floors. Further, $\mathbf{I}_a$ is the identity matrix of dimension a, $\mathbf{0}_{axb}$ is the zero matrix of dimensions axb, $\mathbf{T}_s$ is a transformation matrix defining relative responses between consecutive floors (i.e., a square matrix with dimension n_s with 1 in the diagonal and -1 in the first off-diagonal). Combining Equations (18) and (2) leads to the representation in Equation (3) where

$$\mathbf{x} = \begin{bmatrix} \mathbf{x}_{ss} \\ \mathbf{x}_q \end{bmatrix} \quad \mathbf{A} = \begin{bmatrix} \mathbf{A}_s & \mathbf{E}_s \mathbf{C}_q \\ \mathbf{0}_{n_q x 2n_s} & \mathbf{A}_q \end{bmatrix} \quad \mathbf{B} = \begin{bmatrix} \mathbf{B}_s \\ \mathbf{0}_{n_q x n_d} \end{bmatrix} \quad \mathbf{E} = \begin{bmatrix} \mathbf{0}_{2n_s x 1} \\ \mathbf{E}_q \end{bmatrix} \quad \mathbf{C} = \begin{bmatrix} \mathbf{C}_s & \mathbf{0}_{n_z x n_q} \end{bmatrix} \quad \mathbf{D} = \begin{bmatrix} \mathbf{D}_s & \mathbf{0}_{n_z x n_q} \end{bmatrix} \tag{20}$$

Also, the state connectivity matrix corresponds to

$$\mathbf{L}_d = \begin{bmatrix} \mathbf{0}_{n_d x n_s} & \mathbf{T}_d & \mathbf{0}_{n_d x n_f} \end{bmatrix} \tag{21}$$

Lastly, the state-space matrices of the excitation model used in the case study is

$$\mathbf{A}_q = \begin{bmatrix} 0 & 1 & 0 & 0 \\ -\omega_g^2 & -2\zeta_g\omega_g & 0 & 0 \\ 0 & 0 & 0 & 1 \\ -\omega_g^2 & -2\zeta_g\omega_g & -\omega_f^2 & -2\zeta_f\omega_f \end{bmatrix} \quad \mathbf{E}_q = \begin{bmatrix} 0 \\ 1 \\ 0 \\ 0 \end{bmatrix} \quad \mathbf{C}_q = \sigma_o \begin{bmatrix} -\omega_g^2 & -2\zeta_g\omega_g & \omega_f^2 & 2\zeta_f\omega_f \end{bmatrix} \tag{22}$$

where σ_o is chosen such that the excitation has the desired a_{RMS} intensity.